

Folate-Decorated Hybrid Polymeric Nanoparticles for Chemically and Physically Combined Paclitaxel Loading and Targeted Delivery

Jinfeng Wang,^{†,§} Wenming Liu,^{†,§} Qin Tu,[†] Jianchun Wang,[†] Na Song,[†] Yanrong Zhang,[†] Nan Nie,[†] and Jinyi Wang^{*,†,‡}

Colleges of Science and Veterinary Medicine and Shaanxi Key Laboratory of Molecular Biology for Agriculture, Northwest A&F University, Yangling, Shaanxi 712100, P. R. China

Received October 11, 2010; Revised Manuscript Received November 23, 2010

In this study, folate-functionalized hybrid polymeric nanoparticles (NPs) were prepared as carriers of low water solubility paclitaxel for tumor targeting, which were composed of monomethoxy-poly(ethylene glycol)-*b*-poly(lactide)-paclitaxel (MPEG-PLA-paclitaxel) and D- α -tocopheryl polyethylene glycol 1000 succinate (TPGS)-folate (TPGS-FOL). NPs with various weight ratios of MPEG-PLA-paclitaxel and TPGS-FOL were prepared using a solvent extraction/evaporation method, which can also physically encapsulate paclitaxel. The size, size distribution, surface charge, and morphology of the drug-loaded NPs were characterized using a Zetasizer Nano ZS, scanning electron microscope (SEM), and atomic force microscopy (AFM). The encapsulation and drug loading efficiencies of these polymeric NPs are analyzed using high-performance liquid chromatography (HPLC) at 227 nm. The combination of covalent coupling and physical encapsulation is found to improve the loading of paclitaxel in NPs greatly. The *in vitro* antitumor activity of the drug-loaded NPs is assessed using a standard method of transcriptional and translational (MTT) assays against HeLa and glioma C6 cells. When the cells were exposed to NPs with the same paclitaxel weights, cell viability decreases in relation to the increase in TPGS-FOL in drug-loaded NPs. To investigate drug-loaded NP cellular uptake, the fluorescent dye coumarin-6 is utilized as a model drug and enveloped in NPs with 0 or 50% TPGS-FOL. Confocal laser scanning microscopy (CLSM) analysis shows that cellular uptake is lower for coumarin-6-loaded NPs with 0% TPGS-FOL than those with 50% TPGS-FOL. However, no difference for NIH 3T3 cells with normally expressed folate receptors is found. Results from *in vitro* antitumor activity and cellular uptake assay demonstrate that folic acid promotes drug-loaded NP cellular uptake through folate receptor-mediated endocytosis (RME). All of these results demonstrate that folate-decorated hybrid polymeric NPs are potential carriers for tumor-targeted drug delivery.

Paclitaxel, extracted from the bark of Pacific yew trees, *Taxus brevifolia* is well known because of its highly effective activity against various solid tumors.^{1,2} It has been used to treat various cancers, including ovarian, breast, and nonsmall cell lung cancer, head and neck carcinomas, and so on for many years.^{3–5} Paclitaxel functions by promoting the assembly and stabilization of microtubules that interfere with mitotic spindle function and ultimately arrests cells in the G₂/M phase of mitosis.⁶ Its clinical applications, however, have been hampered by its low water solubility and poor selectivity. The currently available version of paclitaxel is formulated in a vehicle composed of a 50:50 (v/v) mixture of Cremophor EL (polyoxyethylated castor oil) and dehydrated alcohol. Cremophor EL has been reported to cause serious side effects, such as hypersensitivity reactions, nephrotoxicity, neurotoxicity, and cardiotoxicity.⁷

To maintain paclitaxel's high activity against many kinds of cancers and overcome the problems associated with its formulation, new formulations, including liposomes, micelles, and polymeric nanoparticles (NPs), have been created to develop its local drug delivery methods.^{8–14} Among these formulations, polymeric NPs have drawn much attention because of their structure and composition flexibility.^{12,13} Polymeric NPs formed

in aqueous solutions by the self-assembly of the amphiphilic polymer can encapsulate hydrophobic drugs into its hydrophobic core, leaving its hydrophilic parts on the surface.¹⁵ The hydrophilic surface can protect the drug from binding to blood proteins and being absorbed into the reticuloendothelial system (RES), thus keeping the drug in the systemic circulation for a prolonged period of time.¹⁶

Current protocols utilized for paclitaxel loading in polymeric NPs include physical encapsulation^{17,18} and covalent coupling.^{19,20} Physical encapsulation has the advantage of high drug-loading rates. However, the drugs easily leak from NPs when they are delivered to target lesions.²¹ A polymer–paclitaxel conjugate possesses these advantages and removes drug leakages from NPs. However, conjugating the drug into the polymer is limited by efficiency.²² Therefore, developing novel protocols to encapsulate adequately hydrophobic agents into amphiphilic polymer–NPs is necessary for anticancer drug delivery.

Drug-loaded NPs can achieve passive targeting in tumors because of their enhanced permeability and retention effects (EPRs) caused by tumor-associated leaky vasculatures and poor lymphatic drainage.²³ However, NPs accumulated in a solid tumor by passive targeting cannot achieve sufficiently high levels of drug concentrations in the tumor cells because the NPs may release a considerable portion of the drugs before they are absorbed.^{24,25} Only a small amount of NPs can be taken up by tumor cells. To improve targeting efficiency and reduce side effects, introducing targeting molecules, such as folic acid,

* To whom correspondence should be addressed. Tel: + 86-29-870 825 20. Fax: + 86-29-870 825 20. E-mail: jywang@nwsuaf.edu.cn.

[†] Colleges of Science and Veterinary Medicine.

[‡] Shaanxi Key Laboratory of Molecular Biology for Agriculture.

[§] These two authors contributed equally to this work.

monoclonal antibodies (mAb225, etc.), and peptides into NPs is necessary because they could recognize and bind to specific receptors that are unique to cancer cells.^{26–28} Among these targeting molecules, folic acid is a low-weight vitamin that can selectively bind to folate receptors, which are frequently overexpressed on the surfaces of many human cancer cell types but whose presence is highly restricted in most normal tissues.²⁹ Therefore, NPs functionalized with folic acid can specifically promote their cancer cellular uptake through folate receptor-mediated endocytosis (RME).^{30,31}

In this study, we prepare folate-decorated hybrid polymer NPs (FD-NPs) with monomethoxy-poly(ethylene glycol)-*b*-poly(lactide)-paclitaxel (MPEG-PLA-paclitaxel) and *D*- α -tocopheryl polyethylene glycol 1000 succinate folate (TPGS-FOL) for targeted paclitaxel delivery. MPEG-PLA-paclitaxel can self-assemble into NPs because it remains an amphiphilic polymer, even after paclitaxel is chemically conjugated into the MPEG-PLA molecule.²¹ These polymeric NPs could deliver paclitaxel by chemical conjugation and physical encapsulation. TPGS is a nonionic water-soluble derivative of natural vitamin E that has been utilized as a safe and effective form of the vitamin to reverse or prevent vitamin E deficiency.³² Because its structure is composed of a lipophilic alkyl tail and a hydrophilic polar head similar to conventional surface-active agents, it is used as an emulsifier and solubilizer for drug delivery formulations.³³ It can increase drug loading in the preparation of NPs and enhance the absorption of the administrative drug because it can inhibit P-glycoprotein (P-gp) activity, which effluxes drugs, such as adriamycin, paclitaxel, and so on.³⁴

Experimental Section

Materials and Reagents. MPEG, TPGS, and folic acid were purchased from Sigma Aldrich (St. Louis, MO). MPEG was dried for 24 h in a vacuum at room temperature before use. TPGS and folic acid were used without additional purification. L-Lactide was obtained from Jinan Daigang Biomaterial (Shandong, China) and recrystallized three times from ethyl acetate. Paclitaxel was purchased from Xi'an Haohuan Biotech (Xi'an, China). *N*-(3-Dimethylaminopropyl)-*N'*-ethylcarbodiimide (EDC) and *N*-hydroxysuccinimide (NHS) were obtained from GL Biochem. (Shanghai, China). Diglycolic anhydride was purchased from Shanghai Westingarea M&E system (Shanghai, China). Coumarin-6, succinic anhydride, stannous 2-ethyl-hexanoate (Sn(Oct)₂), and 4-(dimethyl amino) pyridine (DMAP) were obtained from J&K Chemical (Logan, UT). MPEG-PLA-paclitaxel and TPGS-FOL utilized in this study were synthesized in our laboratory. (For more detailed information on their synthesis and characterization, see the Supporting Information.) All solvents and other chemicals were purchased from local commercial suppliers and were of analytical reagent grade, unless otherwise stated. All solutions were prepared using ultrapurified water supplied by a Milli-Q system (Millipore).

Preparation of Paclitaxel-Loaded NPs. The paclitaxel-loaded NPs of the MPEG-PLA-paclitaxel and TPGS-FOL blends were prepared by a modified solvent extraction/evaporation method. We use 0, 20, 33.3, and 50% FD-NPs to denote the NPs of 0, 20, 33.3, and 50% TPGS-FOL in the blends of the two conjugates. The weight ratios between MPEG-PLA-paclitaxel and TPGS-FOL in these NPs are thus 1:0, 4:1, 2:1, and 1:1, respectively. We dissolved 3 mg paclitaxel and 15 mg of the MPEG-PLA-paclitaxel and TPGS-FOL blends at various weight ratios in 2 mL of methylene chloride under stirring condition. The blend solution was continuously stirred for 4 h and then added dropwise to 30 mL of water under gentle stirring at room temperature. Afterward, the emulsion was evaporated overnight and then centrifuged at 11 500 rpm for 20 min. The pellet was resuspended in water and freeze-dried for 2 days to get the NPs powder.

Coumarin-6-loaded NPs were prepared using coumarin-6 instead of paclitaxel following the same procedures as those described above.

Characterization. The size distribution and zeta potential of the polymeric NPs were determined by a Zetasizer Nano ZS (Malvern Instruments, Malvern, U.K.) instrument at ambient temperature. The concentration of NP suspension was 0.05 mg/mL. The shapes and sizes of the polymeric NPs were observed at 75 K with a JSM-6701F scanning electron microscope (SEM) as well as with an AJ-III atomic force microscope (AFM, Nano Science Development, Shanghai, China). For AFM studies, a 59 μ m AFM scanner (AJ-III, Nano Science Development) and Si₃N₄ tip (Mikro Masch) were employed for NP scanning. The tip cantilever length was $100 \pm 5 \mu$ m, the width was $35 \pm 3 \mu$ m, the thickness was 1.7 to 2.3 μ m, the resonance frequency was 190–325 kHz, and the force constant was 5.5–22.5 N/m. Image acquisition was carried out using iNanoSPM software (Nano Science Development). Sampling points were set at 256, and the scanning speed was 1.74 kHz.

Drug Encapsulation and Loading Efficiency. The paclitaxel formulated in the NPs was measured by high-performance liquid chromatography (HPLC, Agilent LC1100).³⁵ A total of 2 mg drug-loaded NPs was dissolved in 2 mL of chloroform. Then, 6 mL diethyl ether was added to the solution to precipitate the polymer. The resulting mixture was centrifuged at 11,500 rpm for 30 min. The supernatant was collected into a fresh vial and dried. The dried drug was dissolved in 2 mL of mobile phase (acetonitrile/water 70:30 v/v) and then was injected through a 20 μ L sample loop. The elution rate was 1.0 mL/min. Paclitaxel was detected at 227 nm using ultraviolet (UV) detection. The retention time of paclitaxel was 7.1 min under these conditions.

The drug encapsulation efficiency (EE) and drug loading efficiency (LE) were calculated by the following equations

$$EE(\%) = \frac{\text{the drug amount in nanoparticles}}{\text{the drug feeding at the preparation course}} \quad (1)$$

$$LE(\%) = \frac{\text{the amount of chemically conjugated drug and physically loaded drug}}{\text{the amount of nanoparticles}} \quad (2)$$

In Vitro Drug Release. The in vitro release assay of paclitaxel from NPs was performed in a phosphate-buffered saline solution (PBS, 0.01 M, pH 7.4) at 37 °C. A total of 1 mg drug-loaded NPs was placed in a centrifuge tube and dispersed in 1 mL of PBS. The dispersed solution was incubated in a shaking water bath at 37 °C. After a predetermined amount of time, the tube was taken out and centrifuged at 11 500 rpm for 30 min. The supernatant was carefully obtained for HPLC analysis, and the same volume of fresh PBS was added to the tube to disperse the rest of the pellets. The tube was incubated for continuous release measurements. Released paclitaxel in the supernatant was extracted by 1 mL of methylene chloride. The collected methylene chloride layer was evaporated at room temperature. The dried paclitaxel was dissolved in 2 mL of mobile phase and analyzed by HPLC following the same procedures as those described above.

Cell Culture. Glioma C6 cells, human cervical carcinoma Hela cells, and NIH 3T3 fibroblasts were provided by the Chinese Academy of Sciences (Shanghai, China). Three types of cells were routinely cultured with Dulbecco's modified Eagle's medium (DMEM) supplemented with 10% fetal bovine serum (FBS), 100 units/mL penicillin, and 100 μ g/mL streptomycin in a humidified atmosphere of 5% CO₂ at 37 °C. To maintain cells in the exponential growth phase, they were passaged at a ratio of 1:3 every 3 days. Before use, the cells were trypsinized, resuspended, and then precultured. Caution was used in handling all human biological material.

In Vitro Cytotoxicity of Paclitaxel-Loaded NPs. To evaluate the cell cytotoxicity of paclitaxel-loaded NPs, we performed an MTT (method of transcriptional and translational) assay to measure cell viability.^{36–38} Two types of cancer cells (C6 cells and Hela cells) were each seeded in 96-well plates (Costar, IL) at a cell density of 5×10^4 cells/mL (200 μ L/well). After 24 h of conventional cultivation, the cells

were further incubated for 24 and 48 h in fresh culture media containing pure paclitaxel or various FD-NPs with 0, 20, 33.3, and 50% TPGS-FOL (i.e., 0, 20, 33.3, and 50% FD-NPs). For comparison, three concentration levels of paclitaxel, 2.5, 5, and 25 $\mu\text{g/mL}$, were utilized for pure paclitaxel and FD-NPs. The concentration levels of paclitaxel in the NPs were determined by HPLC and ^1H NMR following methods previously reported.^{35,39} The postreaction culture medium was replaced by both MTT solution (5 mg/mL, 20 μL /well) and supplemented DMEM culture medium (150 μL /well), followed by further culture for 4 h. The supernatant was discarded, and 200 μL of DMSO was added to the wells. The plates were then placed in a shaking incubator (SKY-100B, Sukun Industrial, Shanghai, China) for 10 min. The absorbance values (A) of each well were recorded at 490 nm by a microplate reader (model 680, BIO-RAD). Each experiment was repeated three times. Blank controls were run simultaneously during each experiment. Cell viability was then calculated as

$$\text{cell viability(\%)} = \frac{A_s}{A_c} \times 100 \quad (3)$$

where A_s and A_c are the absorbance values of the sample (i.e., paclitaxel and paclitaxel-loaded NPs) group and control group, respectively.

In Vitro Cellular Uptake of NPs. In vitro cellular uptake assay was performed following the general protocol previously reported.^{36,37} First, cells (C6 cells, Hela cells, and NIH 3T3 cells) were seeded into 96-well plates at a cell density of 5×10^4 cells/mL (200 μL /well). After 24 h of conventional culture, the culture medium was replaced with a suspension of coumarin-6-loaded 0 or 50% FD-NPs with an NP concentration of 200 $\mu\text{g/mL}$. The culture was then incubated for 0.5, 2, 4, and 6 h. The NP suspension in the testing wells was then removed, and the wells were washed three times with PBS (0.01 M, pH 7.4) to remove the nonphagocytosized NPs. A total of 0.5% Triton X-100 in 0.2 mol/L NaOH solution (50 μL /well) was then added to the wells to lyse the cells. Finally, the fluorescence images of coumarin-6-loaded NPs in the desired cells were acquired by an inverted fluorescence microscope (Olympus, CKX41) with a charge-coupled device camera (QIMAGING, Micropublisher 5.0 RTV) and a mercury lamp (Olympus, U-RFLT50) and analyzed using Image-Pro Plus 6.0 (Media Cybernetics, Silver Spring, MD) software. The cellular uptake efficiency was expressed as the percentage of the fluorescence intensity of the testing wells over that of the positive control wells.

For the fluorescence imaging of cellular uptake, C6 cells, Hela cells, and NIH 3T3, cells at a density of 2×10^5 cells/mL were cultivated for 24 h on coverslips in 12-well culture plates (1 mL/well). Suspensions of coumarin-6-loaded 0 or 50% FD-NPs were then added (0.5 mL/well) to the cell culture medium at a concentration of 200 $\mu\text{g/mL}$. Cells were washed three times after incubation for 1 h and then fixed using 4% (v/v) paraformaldehyde aqueous solution. After 10 min of fixing at room temperature, followed by rinsing with PBS, 10 $\mu\text{g/mL}$ propidium iodide (PI) in PBS was added to stain the nuclei for 5 min. The dyed cells were finally washed with PBS and then observed by a CLSM (Zeiss LSM5 Pascal).

Statistical Analysis. Statistical analysis was performed via analysis of variance using SPSS 12.0 (SPSS, Inc.) software. Data for each experiment were presented as means \pm standard deviation (SD). Differences among means were tested using Duncan's multiple range tests. A p value of 0.05 was considered to be statistically significant.

Results and Discussion

Preparation of Drug-Loaded Polymeric NPs and Assay of Drug-Loading Level. Although many efforts have been devoted to embed physically or couple covalently paclitaxel to polymeric NPs,^{17–20} few researches on physical and covalent combinations have been conducted to increase paclitaxel in polymeric NPs and targeted delivery. In this study, we first

synthesized the amphiphilic polymer MPEG-PLA, to which paclitaxel was then covalently conjugated. We then used this material as a carrier to encapsulate physically paclitaxel in the presence of TPGS-FOL. The processes are as follows. First, MPEG-PLA-paclitaxel, TPGS-FOL, as well as paclitaxel were dissolved in methylene chloride. These were then added dropwise to water under gentle stirring. The polymer in this process self-assembled into internal hydrophobic and external hydrophilic nanostructures. The hydrophobic paclitaxel was simultaneously encapsulated into the nanostructure through similar compatibilities of esters by other esters as well as hydrogen bonds. According to previous reports,³³ TPGS, an emulsifier, can increase the rate of drug loading in the nanostructures. To determine further the effect of TPGS on the drug-loading rate, we prepared four polymeric NPs with different TPGS ratios (i.e., 0, 20, 33.3, and 50% FD-NPs). Table S2 (Supporting Information) shows the drug-loading rates of these NPs, which indicates that TPGS-FOL-containing NPs possess higher physical entrapment abilities compared with non-TPGS-FOL NPs. However, when the TPGS-FOL content in the NPs was increased from 20 to 33.3%, physical entrapment efficiency of paclitaxel decreased by 1.33%; when the TPGS-FOL content in the NPs was increased to 50%, paclitaxel physical entrapment efficiency decreased by 2.49%. An increase in TPGS-FOL content reduces the physical entrapment of drugs. This may be because increases in TPGS-FOL content cause NP hydrophilicities to strengthen, which is not conducive to the physical embedding hydrophobic paclitaxel.³⁸ The results indicate that drug physical entrapment rates are highest when the TPGS-FOL content in NPs is 20%. In the current study, however, the drug-loaded NPs included not only physically entrapped paclitaxel but also covalently conjugated paclitaxel. The decrease in TPGS-FOL content in the NPs means an increase in MPEG-PLA-paclitaxel levels. After a comprehensive comparison, the drug-loading rate was found to be highest when the TPGS-FOL content in the NPs was 33.3% rather than when the TPGS-FOL content was 20%. Therefore, drug-loaded NPs prepared using 33.3% TPGS-FOL were employed for the next study.

Size, Morphology, and Zeta Potential of Polymeric NPs. The sizes and size distributions of drug-loaded polymeric NPs were characterized using a Zetasizer Nano ZS instrument. The results (Figure 1 and Table S3 of the Supporting Information) show no obvious differences among the four dosage forms. The average diameter of the drug-loaded polymeric NPs was ~ 300 nm. To investigate the shape of the drug-loaded polymeric NPs, the morphology of 33.3% FD-NPs was visualized by SEM and AFM as an example (Figure 1), demonstrating that drug-loaded polymeric NPs were dispersed as individual particles with regular spherical shapes. In addition, the diameters of the NPs obtained by SEM and AFM were in the range of the diameters obtained using Zetasizer Nano ZS. Analysis of the zeta potential of paclitaxel-loaded NPs in PBS showed that all NP formulations had negative surface charges at room temperature (Supporting Information, Table S3). The NPs showed no aggregation in the SEM and AFM images, which is attributed to the hydrophilic nature and negative surface charges of the NPs.

In Vitro Drug Release. The assay of in vitro drug release aimed to quantify the cumulative percentage release of paclitaxel from the four dosage forms (i.e., 0, 20, 33.3, and 50% FD-NPs) under simulated physiological conditions (PBS, pH 7.4, at 37 $^\circ\text{C}$) over an extended period of time. HPLC analysis (Supporting Information, Figures S4–S6) showed that in vitro drug release of all drug-loaded NPs exhibited a biphasic release, with a slight burst release in the first stage, followed by a period of sustained release

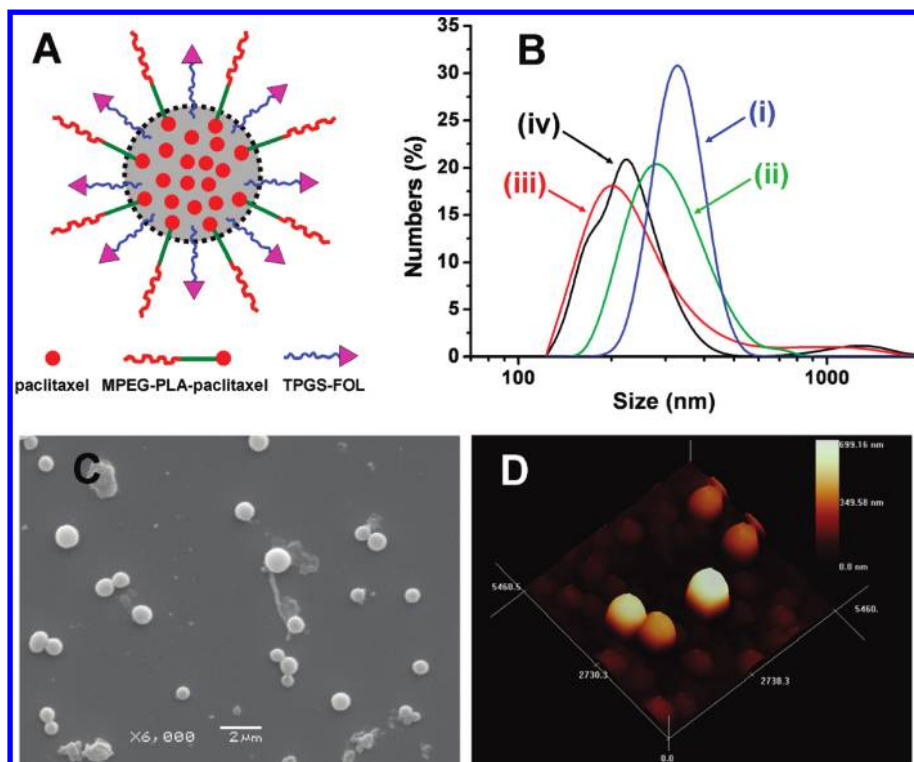


Figure 1. (A) Schematic representation of paclitaxel physically and covalently loaded NPs of the MPEG-PLA-paclitaxel and TPGS-FOL blend. (B) Hydrodynamic size distribution of four NP formulations: (i) 0% FD-NPs, (ii) 20% FD-NPs, (iii) 33.3% FD-NPs, and (iv) 50% FD-NPs. (C) SEM image of 33.3% FD-NPs. (D) AFM image of 33.3% FD-NPs.

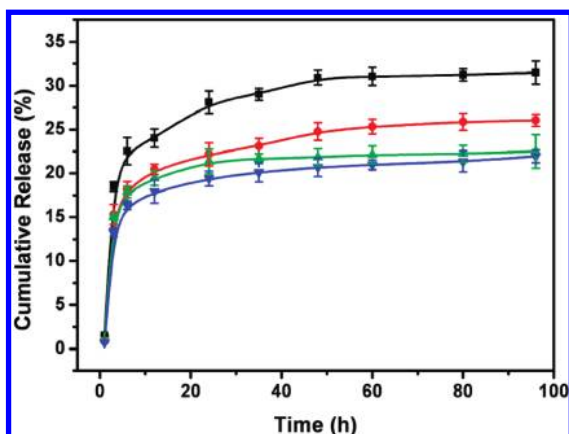


Figure 2. Release profile of paclitaxel from FD-NPs in PBS (pH 7.4) containing 0.1% w/v Tween 80 at 37 °C. Data represents mean \pm SD ($n = 3$). (i) 0% FD-NPs, (ii) 20% FD-NPs, (iii) 33.3% FD-NPs, and (iv) 50% FD-NPs.

(Figure 2). In the first 3 h, the initial burst release is not above 20% (18.5, 15.34, 15.01, and 13.29% for 50, 33.3, 20, and 0% FD-NPs, respectively). This was mainly due to the release of physically entrapped paclitaxel but may also be attributed to the release of paclitaxel molecules located within the hydrophilic shell. Continuous and sustained releases occurred (Supporting Information, Figure S6), indicating that paclitaxel was well-entrapped in the NPs and that the chemically coupled drug may have been hydrolyzed from the polymer conjugate and slowly released at the same time.²¹ After 96 h, 31.03, 25.93, 22.8, and 22.45% of the entrapped paclitaxel was released from 50, 33.3, 20, and 0% FD-NPs, respectively. Higher releases of paclitaxel correspond to the higher TPGS-FOL contents in the NPs. This may be because hydrophilic TPGS-FOL allows water to permeate easily into the NPs. As such, drug release was faster.³⁶ In addition, the drug released from 50% FD-NPs was far higher than that released from the three other dosage forms

because these NPs had the highest amount of the physically entrapped drug.

In Vitro Cytotoxicity of Paclitaxel-Loaded NPs. The efficiency of the four paclitaxel-loaded NPs on the viability of C6 cells and Hela cells was assessed using standard MTT assays.^{37,38} For each kind of NP, three NP samples with varying paclitaxel concentrations (2.5, 5, and 25 $\mu\text{g}/\text{mL}$) were examined by HPLC and ^1H NMR following the methods reported previously.^{33,39} These were chosen for their quantitative cytotoxicity based on clinical drug dosages.³⁸ Meanwhile, control experiments were performed using pure paclitaxel for each test.

The results show (Figure 3) that C6 cell viability after 24 h of pure paclitaxel treatment using 2.5, 5, and 25 $\mu\text{g}/\text{mL}$ of paclitaxel were 79.18 ± 2.63 , 77.02 ± 3.85 , and $59.68 \pm 2.86\%$, respectively. When the treatment time reached 48 h for the same drug concentrations, the cell viability decreased to 73.30 ± 4.21 , 70.64 ± 5.02 , and $39.64 \pm 2.41\%$, respectively. Higher paclitaxel concentrations and longer treatment times result in the higher mortality of C6 cells, which means lower cell viability and higher anticancer efficiency. Similar results were also obtained for Hela cells treated with pure paclitaxel. Hela cells seemed more vulnerable than C6 cells when they were exposed to the same paclitaxel concentrations. After 24 and 48 h treatments, the viability of Hela cells decreased from 87.07 ± 2.17 (2.5 $\mu\text{g}/\text{mL}$), 50.33 ± 2.83 (5 $\mu\text{g}/\text{mL}$), and $39.97 \pm 2.59\%$ (25 $\mu\text{g}/\text{mL}$) to 39.85 ± 3.56 , 33.29 ± 3.15 , and $25.61 \pm 3.54\%$, respectively.

Compared with pure paclitaxel cytotoxicity in C6 and Hela cells, drug-loaded NP formulations exhibited higher toxicity to the applied cancer cell types (Figure 3). For example, the viability of 20% FD-NPs to C6 and Hela cells following the same treatment as pure paclitaxel decreased from 71.01 ± 2.15 (2.5 $\mu\text{g}/\text{mL}$), 69.39 ± 3.35 (5 $\mu\text{g}/\text{mL}$), and $51.56 \pm 3.33\%$ (25 $\mu\text{g}/\text{mL}$) to 55.59 ± 3.85 , 54.04 ± 2.15 , $36.60 \pm 3.19\%$, respectively, and from 79.41 ± 2.67 , 43.01 ± 3.51 , and $28.26 \pm 2.94\%$ to 37.40 ± 2.36 , 29.19

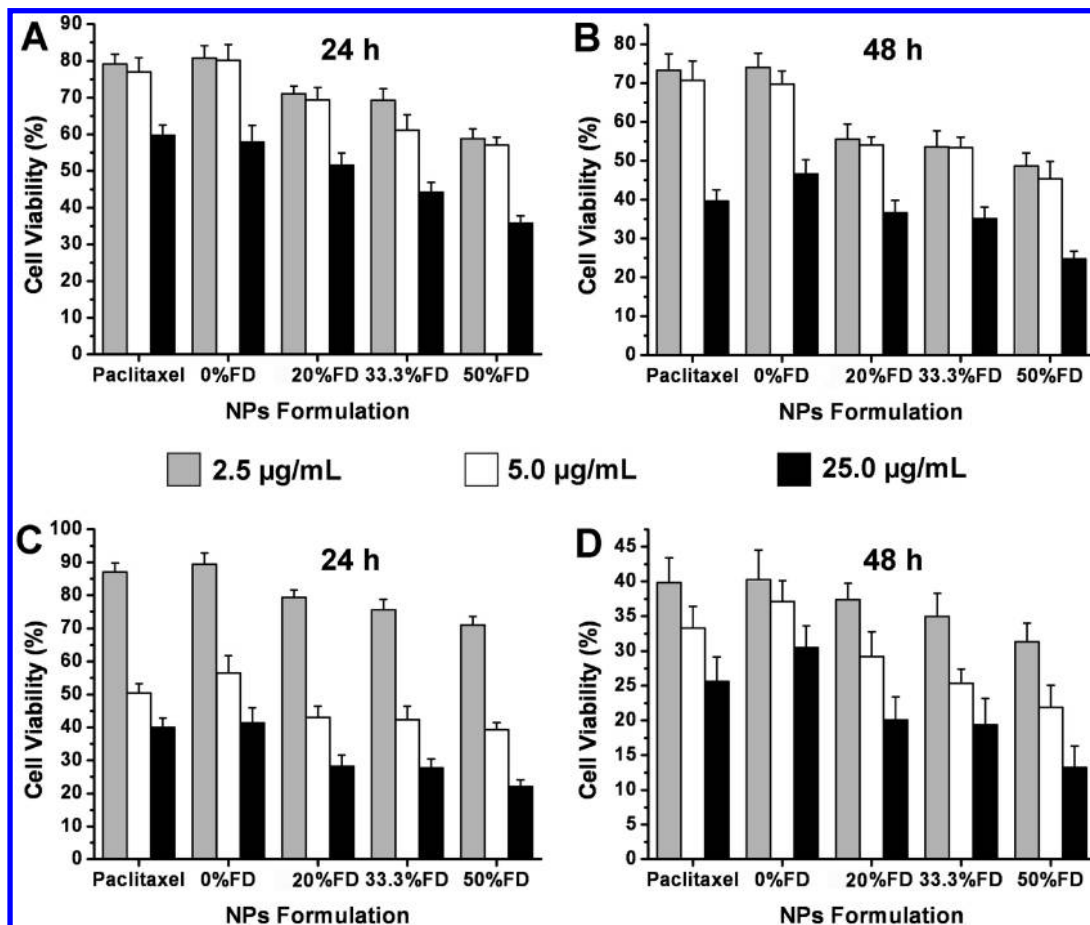


Figure 3. Cell viability of C6 cells and Hela cells treated with paclitaxel and various paclitaxel-loaded FD-NPs (i.e., 0, 20, 33.3, and 50% FD-NPs). Three paclitaxel concentrations (2.5, 5, and 25 $\mu\text{g/mL}$) were used here. (A) C6 cells 24 h after treatment. (B) C6 cells 48 h after treatment. (C) Hela cells 24 h after treatment. (D) Hela cells 48 h after treatment.

± 3.57 , and $20.05 \pm 3.34\%$ for the same paclitaxel concentrations, respectively. The results suggest that the amount of the folate component could affect the cytotoxic ability of paclitaxel-loaded NPs to cancer cells (i.e., the lethality of cancer cells) because they appeared to be positively related to the concentration of NP formulations, aside from paclitaxel concentration and treatment time. As shown in Figure 3, the viability of 50% FD-NPs to C6 cells and Hela cells is lower than that of 0, 20, and 33.3% FD-NPs after 24 and 48 h treatments, decreasing from 58.76 ± 2.67 (2.5 $\mu\text{g/mL}$), 57.06 ± 2.17 (5 $\mu\text{g/mL}$), and $35.78 \pm 2.05\%$ (25 $\mu\text{g/mL}$) to 48.68 ± 3.35 , 45.39 ± 4.39 , and $24.69 \pm 2.05\%$ and from 70.94 ± 2.37 (2.5 $\mu\text{g/mL}$), 39.25 ± 2.05 (5 $\mu\text{g/mL}$), and $22.12 \pm 2.41\%$ (25 $\mu\text{g/mL}$) to 31.32 ± 2.67 , 21.91 ± 3.18 , and $13.24 \pm 3.08\%$, respectively. The highest lethality of cancer cells occurred at the highest concentration of NP formulations after treatment and for the longest period of time. The orders of all C6 and Hela cell viabilities examined to different drug-loaded NPs were 50% FD-NPs > 33.3% FD-NPs > 20% FD-NPs > 0% FD-NPs. The results demonstrate that the cytotoxicity of paclitaxel-loaded NPs to cancer cells was improved by the folate component, which has been reported to bind to folate receptors with high affinity, thus mediating in cellular uptake via RME.^{30,31,37}

In Vitro Cellular Uptake of NPs. To investigate folate-targeting cellular uptake, a short-term particle endocytosis test was visually carried out using coumarin-6-loaded FD-NPs. The formulation of 50% FD-NPs was applied because it had the highest folate component among all of the NPs and therefore the best cytotoxicity. The results show (Figure 4) that coumarin-6-loaded NPs (green fluorescent dots in Figure 4) penetrated

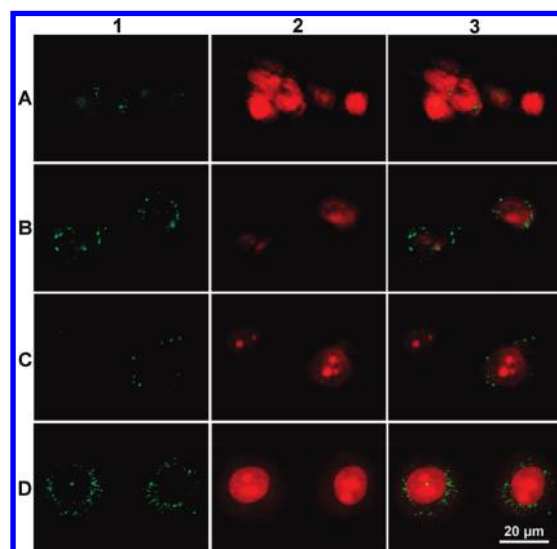


Figure 4. Confocal laser scanning microscopy images showing the internalization of fluorescent NPs in cells (1 h incubation). Column 1: FITC channels showing green fluorescence from coumarin-6-loaded NPs distributed in the cytoplasm. Column 2: PI channels showing red fluorescence from propidium iodide-stained nuclei. Column 3: Merged channels of FITC and PI. Rows A and B: C6 cells. Rows C and D: Hela cells. In Rows A and C, folate-free NPs were used, whereas in Rows B and D, folate NPs were used.

the cells and were mostly distributed around the nucleus (i.e., in the cytoplasm). Furthermore, fluorescent dots in samples incubated with 50% FD-NPs in C6 cells and Hela cells were

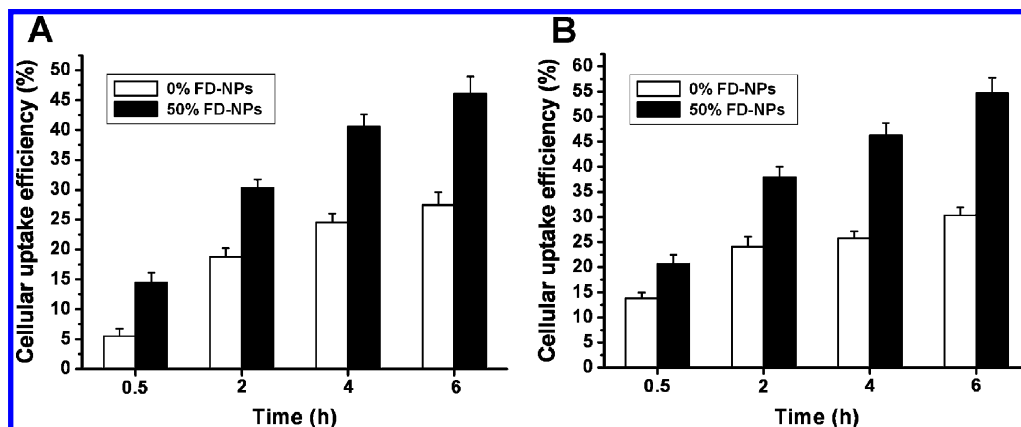


Figure 5. (A) C6 and (B) Hela cell uptake efficiency of coumarin-6-loaded 0% FD-NPs (i.e., folate-free NPs) or 50% FD-NPs at an NP concentration of 200 $\mu\text{g}/\text{mL}$ for 0.5, 2, 4, and 6 h treatment.

more concentrated than those with 0% FD-NPs. The images visually demonstrate folate's improved effect on cellular uptake, which could also be a possible explanation for FD-NPs' higher cytotoxicity to C6 and Hela cells. The results show that RME promotes the penetration of FD-NPs, whereas folate binds to overexpressed folate receptors on C6 and Hela cells. As a control, a normal cell type, NIH 3T3, was also utilized in this test. Folate receptors in such cells have been demonstrated to be normally expressed.⁴⁰ The results (Supporting Information, Figure S7) show that the difference in fluorescent dots in the cytoplasm of NIH 3T3 cells was not significant between 0 and 50% FD-NPs incubation.

To analyze further the degree of folate-assisted endocytosis and to better control folate-assisted cancer cell uptake, we performed a quantitative cellular uptake test on C6 and Hela cells using coumarin-6-loaded 0 and 50% FD-NPs. Four incubation times (0.5, 2, 4, and 6 h) were chosen according to the normal sequential research procedures.^{37,38} The results show (Figure 5) that the cellular uptake of NPs in cancer cells increased with increasing incubation times. The cellular uptake efficiency of 50% FD-NPs in cancer cells was clearly higher than that of 0% FD-NPs. For example, after 0.5 and 6 h incubation, the cellular uptake efficiency of 50% FD-NPs in C6 cells was 14.46 ± 1.66 and $46.03 \pm 2.91\%$, respectively. However, those of 0% FD-NPs in C6 cells were only 5.49 ± 1.24 and $27.41 \pm 2.20\%$, respectively. Meanwhile, the cellular uptake efficiency of 50% FD-NPs in Hela cells was 20.63 ± 1.82 and $54.71 \pm 3.05\%$, respectively, and that of 0% FD-NPs was only 13.78 ± 1.15 and $30.35 \pm 1.65\%$, respectively. These results demonstrate that folate can quickly improve the endocytosis of cancer cells, which could be disastrous for specific tumors (i.e., those with overexpressed folate receptors) because of more-efficient targeted attacks from anticancer drug-loaded NPs.

Conclusions

In this study, we synthesized and characterized two polymers, MPEG-PLA-paclitaxel and TPGS-FOL, and four types of NPs with various weight ratios of MPEG-PLA-paclitaxel to TPGS-FOL. Meanwhile, paclitaxel was physically encapsulated in these NPs. These polymers were successfully prepared as new carriers for tumor-targeted drug delivery. HPLC analysis showed that the combination of physical encapsulation and covalent coupling greatly improved the loading of paclitaxel in NPs. The mean diameters of the four NP formulations characterized by Zetasizer Nano

ZS are not obviously different (~ 300 nm), and their surfaces all had negative charge in PBS (pH 7.4). Taking 33.3% FD-NPs as an example, SEM and AFM experiments showed that the NP formulations have individual particles and regular shapes. The in vitro cytotoxicity assay of the drug-loaded FD-NPs showed that NPs with larger folate components had higher cytotoxicity to cancer cells. The cytotoxicity of all drug-loaded FD-NPs to cancer cells was higher than that of the pristine drug with the same paclitaxel concentration. Confocal imaging qualitative and quantitative assays reveal that coumarin-6-loaded 50% FD-NPs had greater cellular uptake compared with coumarin-6 loaded 0% FD-NPs. However, no obvious difference was found when these NPs were compared with normal cells. The results suggest that polymeric NP formulations are superior to the pristine drug in many aspects, and folate-decorated NPs could be efficiently absorbed by cancer cells through the mechanism of folate-RME. This study shows that folate-decorated hybrid polymeric NPs are potential carriers for tumor-targeted drug delivery. To demonstrate further its function, in vivo studies on the folate-decorated hybrid polymeric NPs are all under the way in our laboratory.

Acknowledgment. This work was supported by the National Natural Science Foundation of China (nos. 209 750 82 and 207 750 59), the Ministry of Education of the People's Republic of China (no. NCET-08-0464), and Northwest A&F University.

Supporting Information Available. Results and discussion on the synthesis and characterization of MPEG-PLA-paclitaxel conjugate and TPGS-FOL. This material is available free of charge via the Internet at <http://pubs.acs.org>.

References and Notes

- Lee, K. H.; Yim, E. K.; Kim, C. J.; Namkoong, S. E.; Um, S. J.; Park, J. S. *Gynecol. Oncol.* **2005**, *98*, 45–53.
- Huizing, M. T.; Sewberath, M. V. H.; Pieters, R. C.; Bok Veenhof, C. H. N.; Vermorken, J. B.; Pinedo, H. M.; Beijnen, J. H. *Cancer Invest.* **1995**, *13*, 381–404.
- Lopes, N. M.; Adams, E. G.; Pitts, T. W.; Bhuyan, B. K. *Cancer Chemother. Pharmacol.* **1993**, *32*, 235–242.
- Rowinsky, E. K.; Cazenave, L. A.; Donehower, R. C. *J. Natl. Cancer Inst.* **1990**, *82*, 1247–1259.
- Wall, M. E.; Wani, M. C. *Cancer Res.* **1995**, *55*, 753–760.
- Costa, M. A.; Simon, D. I. *Circulation* **2005**, *111*, 2257–2273.
- Liebmann, J.; Cook, J. A.; Mitchell, J. B. *Lancet* **1993**, *342*, 1428–1428.
- Saad, M.; Garbuzenko, O. B.; Ber, E.; Chandna, P.; Khandare, J. J.; Pozharov, V. P.; Minko, T. *J. Controlled Release* **2008**, *130*, 107–114.

- (9) Schmitt-Sody, M.; Strieth, S.; Krasnici, S.; Sauer, B.; Schulze, B.; Teifel, M.; Michaelis, U.; Naujoks, K.; Dellian, M. *Clin. Cancer Res.* **2003**, *9*, 2335–2341.
- (10) Zhang, C.; Qu, G. W.; Sun, Y. J.; Wu, X. J.; Yao, Z. L.; Guo, Q. L.; Ding, Q.; Yuan, S.; Shen, Z.; Ping, Q.; Zhou, H. *Biomaterials* **2008**, *29*, 1233–1241.
- (11) Park, E. K.; Kim, S. Y.; Lee, S. B.; Lee, Y. M. *J. Controlled Release* **2005**, *109*, 158–168.
- (12) Patil, Y. B.; Toti, U. S.; Khair, A.; Ma, L.; Panyam, J. *Biomaterials* **2009**, *30*, 859–866.
- (13) Keresztessy, Z.; Bodnar, M.; Ber, E.; Hajdu, I.; Zhang, M.; Hartmann, J. F. *Colloid Polym. Sci.* **2009**, *287*, 759–765.
- (14) Kim, S. Y.; Lee, Y. M. *Biomaterials* **2001**, *22*, 1697–1704.
- (15) Liu, L. H.; Guo, K.; Lu, J.; Venkatraman, S. S.; Luo, D.; Ng, K. C.; Ling, E. A.; Mochhala, S.; Yang, Y. Y. *Biomaterials* **2008**, *29*, 1509–1517.
- (16) Gref, R.; Luck, M.; Quellec, P.; Marchand, M.; Dellacherie, E.; Harnisch, S.; Blunk, T.; Müller, R. H. *Colloids Surf., B* **2000**, *18*, 301–313.
- (17) Kim, J. H.; Kim, Y. S.; Kim, S.; Park, J. H.; Kim, K.; Choi, K.; Chung, H.; Jeong, S. Y.; Park, R. W.; Kim, I. S.; Kwon, I. C. *J. Controlled Release* **2006**, *111*, 228–234.
- (18) Hu, Y.; Xie, J. W.; Tong, Y. W.; Wang, C. H. *J. Controlled Release* **2007**, *118*, 7–17.
- (19) Tong, R.; Yala, L. D.; Fan, T. M.; Cheng, J. J. *Biomaterials* **2010**, *31*, 3043–3053.
- (20) Vemula, P. K.; Cruikshank, G. A.; Karp, J. M.; John, G. *Biomaterials* **2009**, *30*, 383–393.
- (21) Xie, Z.; Guan, H. L.; Chen, X.; Lu, C.; Chen, L.; Hu, X.; Shi, Q.; Jing, X. *J. Controlled Release* **2007**, *117*, 210–216.
- (22) Xie, Z. G.; Lu, T. C.; Chen, X. S.; Lu, C. H.; Zheng, Y. H.; Jing, X. B. *J. Appl. Polym. Sci.* **2007**, *105*, 2271–2279.
- (23) Ulbrich, K.; Subr, V. *Adv. Drug Delivery Rev.* **2004**, *56*, 1023–1050.
- (24) Brigger, I.; Dubernet, C.; Couvreur, P. *Adv. Drug Delivery Rev.* **2002**, *54*, 631–651.
- (25) Choi, K. Y.; Chung, H.; Min, K. H.; Yoon, H. Y.; Kim, K.; Park, J. H.; Kwon, I. C.; Jeong, S. Y. *Biomaterials* **2010**, *31*, 106–114.
- (26) Prabakaran, M.; Grailer, J. J.; Pilla, S.; Steeber, D. A.; Gong, S. Q. *Biomaterials* **2009**, *30*, 3009–3019.
- (27) Lin, J. J.; Chen, J. S.; Huang, S. J.; Ko, J. H.; Wang, Y. M.; Chen, T. L.; Wang, L. F. *Biomaterials* **2009**, *30*, 5114–5124.
- (28) Liu, P.; Li, Z.; Zhu, M.; Sun, Y.; Li, Y.; Wang, H.; Dwan, Y. *J. Mater. Sci.: Mater. Med.* **2010**, *21*, 551–556.
- (29) Zhao, H. Z.; Yue, L.; Yung, L. *Int. J. Pharm.* **2008**, *349*, 256–268.
- (30) Leamon, C. P.; Reddy, J. A. *Adv. Drug Delivery Rev.* **2004**, *56*, 1127–1141.
- (31) Park, E. K.; Lee, S. B.; Lee, Y. M. *Biomaterials* **2005**, *26*, 1053–1061.
- (32) Mu, L.; Seow, P. H. *Colloids Surf., B* **2006**, *47*, 90–97.
- (33) Zhang, Z. P.; Feng, S. S. *Biomaterials* **2006**, *27*, 262–270.
- (34) Varma, M. V. S.; Sateesh, K.; Panchagnula, R. *Mol. Pharm.* **2005**, *2*, 12–21.
- (35) Ruan, G.; Feng, S. S. *Int. J. Pharm.* **2003**, *24*, 5037–5044.
- (36) Zhang, Z. P.; Lee, S. H.; Feng, S. S. *Biomaterials* **2007**, *28*, 1889–1899.
- (37) Liu, Y.; Li, K.; Pan, J.; Liu, B.; Feng, S. S. *Biomaterials* **2010**, *31*, 330–338.
- (38) Pan, J.; Feng, S. S. *Biomaterials* **2008**, *29*, 2663–2672.
- (39) Zhang, X. F.; Li, Y. X.; Chen, X. S.; Wang, X. H.; Xu, X. Y.; Liang, Q. Z.; Hu, J.; Jing, X. *Biomaterials* **2005**, *26*, 2121–2128.
- (40) Parker, N.; Turk, M. J.; Westrick, E.; Lewis, J. D.; Low, P. S.; Leamon, C. P. *Anal. Biochem.* **2005**, *338*, 284–293.

BM101206G